

AD-A056 139

INDIANA UNIV AT BLOOMINGTON DEPT OF CHEMISTRY

F/G 20/9

DEVELOPMENT AND CHARACTERIZATION OF A MINIATURE INDUCTIVELY COU--ETC(U)

JUL 78 R N SAVAGE, G M HIEFTJE

N00014-76-C-0838

UNCLASSIFIED

13

NL

1 OF 1  
AD  
A056 139



**LEVEL II**

AD A056139

AD No. \_\_\_\_\_  
DDC FILE COPY

REPORT DOCUMENTATION PAGE		READ INSTRUCTIONS BEFORE COMPLETING FORM
1. REPORT NUMBER	2. GOVT ACCESSION NO.	3. REPORT TYPE AND CATALOG NUMBER
Thirteen	(12)	
4. TITLE (and Subtitle)		5. TYPE OF REPORT & PERIOD COVERED
Development and Characterization of a Miniature Inductively Coupled Plasma Source for Atomic Emission Spectrometry.		Interim Technical Report
6. AUTHOR(s)		7. PERFORMING ORG. REPORT NUMBER
(10) R. N. Savage G. M. Hieftje		NR 051-622
8. CONTRACT OR GRANT NUMBER(s)		9. PROGRAM ELEMENT, PROJECT, TASK AREA & WORK UNIT NUMBERS
(15) N00014-76-C-0838		NR 051-622
10. PERFORMING ORGANIZATION NAME AND ADDRESS		11. REPORT DATE
Department of Chemistry Indiana University Bloomington, Indiana 47401		July 3, 1978
12. CONTROLLING OFFICE NAME AND ADDRESS		13. NUMBER OF PAGES
Office of Naval Research Washington, D.C.		29
14. MONITORING AGENCY NAME & ADDRESS (if different from Controlling Office)		15. SECURITY CLASS. (of this report)
(11) 3 Jul 78		Unclassified
16. DISTRIBUTION STATEMENT (of this Report)		15a. DECLASSIFICATION/DOWNGRADING SCHEDULE
Approved for public release; distribution unlimited (14) 13 (12) 34 p.		
17. DISTRIBUTION STATEMENT (of the abstract entered in Block 20, if different from Report)		
Prepared for publication in ANALYTICAL CHEMISTRY		
18. SUPPLEMENTARY NOTES		
19. KEY WORDS (Continue on reverse side if necessary and identify by block number)		
86/MIN		
20. ABSTRACT (Continue on reverse side if necessary and identify by block number)		
<p>A miniature inductively coupled plasma source for atomic emission spectrometry is described and a preliminary evaluation of its analytical capabilities is presented. The mini-ICP is very economical to sustain and works well with less than 1 kW of RF power and 8 L min<sup>-1</sup> of argon coolant gas. In addition, the new source possesses some unique operating characteristics which simplify sample introduction. In this paper, detection limits, multi-element capabilities, and other analytical features of the mini-ICP are compared with those</p> <p>(continued)</p>		

DDC  
JUL 12 1978  
F

78.07 07 082476 685

UNCLASSIFIED

SECURITY CLASSIFICATION OF THIS PAGE (When Data Entered)

← demonstrated by a conventional ICP source and shown to be comparable. In addition, the two plasmas are shown to exhibit similar excitation temperatures in the respective analyte observation regions (i.e., plasma tail flames). These results suggest that the mini-ICP possesses the same desirable atomization and excitation characteristics as conventional ICP sources.

X

ADMISSION BY	
NTIS	White Section <input checked="" type="checkbox"/>
DDG	Unit Section <input type="checkbox"/>
UNANNOUNCED	<input type="checkbox"/>
JUSTIFICATION	
BY	
DISTRIBUTION/AVAILABILITY CODES	
Dist	AVAIL. NO. OF SPECIAL
A	

78 07 07 082

UNCLASSIFIED

SECURITY CLASSIFICATION OF THIS PAGE (When Data Entered)



DEVELOPMENT AND CHARACTERIZATION OF A MINIATURE INDUCTIVELY  
COUPLED PLASMA SOURCE FOR ATOMIC EMISSION SPECTROMETRY

R. N. Savage and G. M. Hieftje\*

Department of Chemistry  
Indiana University  
Bloomington, Indiana 47401



# BRIEF

~~~~~

A new miniature inductively coupled plasma source operates at low RF power levels and requires less argon support gas than conventional ICP sources, but exhibits many of the same analytical capabilities.

# ABSTRACT

~~~~~

A miniature inductively coupled plasma source for atomic emission spectrometry is described and a preliminary evaluation of its analytical capabilities is presented. The mini-ICP is very economical to sustain and works well with less than 1 kW of RF power and 8 L min<sup>-1</sup> of argon coolant gas. In addition, the new source possesses some unique operating characteristics which simplify sample introduction. In this paper, detection limits, multi-element capabilities, and other analytical features of the mini-ICP are compared with those demonstrated by a conventional ICP source and shown to be comparable. In addition, the two plasmas are shown to exhibit similar excitation temperatures in the respective analyte observation regions (i.e., plasma tail flames). These results suggest that the mini-ICP possesses the same desirable atomization and excitation characteristics as conventional ICP sources.

During the past decade the radio-frequency inductively coupled plasma (ICP) has emerged as a very promising excitation source for atomic emission spectrometry (AES) and many investigators have examined both the physical nature (1-4) and analytical capabilities (5-7) of ICP sources for simultaneous multi-element optical emission analysis. However, one of the main impediments to the acceptance of these ICP-AES systems has been the high operational cost and complexity associated with the ICP source itself. In addition, the high power RF equipment required by conventional ICP sources increases their initial cost, requires a lot of laboratory space and can produce strong radio-frequency interference (RFI), unless proper shielding techniques are employed.

Many of these limitations should be overcome merely by shrinking the physical dimensions of the ICP. Such a mini-ICP, if operated at similar power densities as its larger counterpart, should exhibit the same high sensitivity, working curve linearity, and freedom from interferences; these desirable features are largely a result of high plasma temperature, which is itself a function of power density (8). In turn, the smaller ICP would require a lower input power to maintain equivalent power density and would consume less coolant gas (argon) during operation. Attendant savings in the cost of the RF power supply, impedance matching device, and transmission lines would be expected. In addition, lower power requirements would reduce necessary laboratory space and expected interference from radiated RF energy.



In the present study, such a mini-ICP was designed, tested, and compared to a larger, conventional plasma. It was found that torch design was particularly critical in the stable formation of the smaller plasma, and hydrodynamic techniques were devised (9) to aid in torch development. Significantly, the plasma supported by the new mini-torch appears both stabler and easier to ignite than its larger brother. Also, detection limits attained with the smaller plasma are comparable to those exhibited by the conventional system, despite excitation temperatures which are slightly lower. Finally, background spectra and multielement detection capabilities of the two plasmas were compared, proving the viability of the new mini-ICP for efficient low-cost routine analyses.

## EXPERIMENTAL

### Instrumentation

A schematic diagram of the apparatus used in this study is shown in Figure 1. Details concerning the individual components are summarized below.

**RF Power System.** RF power is developed by a crystal-controlled air-cooled power amplifier (Model HFP-2500 D with Model APCS-1 power control, Plasma-Therm Inc., Kresson, N.J.) operating at 27.12 MHz. The RF power is continuously variable up to a maximum of 2.5 kW and is transmitted via a coaxial cable (RG 8/U) to the load coil of an automatic impedance matching unit (Model AMN-2500E, Plasma-Therm Inc., Kresson, N.J.). The water-cooled load coils are fabricated of 1/8" (3.175mm) O.D. copper tubing. For mini-ICP operation a 2-turn load coil with a diameter of  $\sim 2$  cm is used; when operating the maxi-ICP a 3-turn coil is employed with a diameter of  $\sim 3$  cm. Primary ignition of the plasma is accomplished by applying to the torch a spark from a tesla coil.

**Torch, Nebulizer and Housing.** In general, the mini-ICP torch has the same features and operates on the same basic principles as conventional ICP torches (10-15). However, the mini-torch is 33% smaller than conventional torches (16,17) and possesses some unique features, as revealed in the diagram of Figure 2. In this diagram, dimensions of the torch are given and its orientation with respect to the load coil is shown. A quartz bonnet, positioned around the end of the torch, aids in electrically screening the conductive plasma gases from the load coil.

Both the plasma and coolant gases (high-purity argon) are introduced tangentially into the torch. The angle at which the gases are introduced is critical and was established empirically using hydrodynamic techniques (9). In addition, the gas inlet tubes were constricted to increase the swirl velocity of the gases as they spiral up the torch. With this technique a stable vortex is formed at low gas flows; a similar effect has been examined in some detail by Barnes (19). A mini-torch employing this design can stably support a plasma using less than  $8 \text{ L min}^{-1}$  of argon coolant gas.

The shape and position of the central injection tube plays a critical role in assuring that the sample is directed into the hottest part of the plasma. In our torch, the injection tube is tipped with a length of capillary tubing adequate to create a laminar flow (19) of exiting sample aerosol. This laminar flow readily penetrates the plasma and reduces the chances of sample being swept around the plasma periphery. A laminar flow design of this nature also enables the injection tube to be positioned as far as 2mm below the end of the plasma tube, where the chances of its overheating and melting are reduced.

The internal diameter of the injection tube is also important because it determines the size of the hole that is punched through the plasma. This hole should be kept small to ensure that the sample channel is electrically screened from the energy addition region (defined as the skin depth) of the plasma (12), and that the sample flow cools the plasma as little as possible. Under these conditions, the addition of sample to the plasma will cause only minimal variations in the plasma's impedance and not affect materially the plasma's stability. This consideration is particularly important in the mini-ICP since the energy addition region occupies a large portion of the



plasma. In this study, excellent plasma stability was obtained using a 0.75mm I.D. capillary injection tube.

The sample introduction system consists of a simple concentric pneumatic nebulizer attached to a dual-tube spray chamber, similar to the one described by Fassel (16). Ordinarily, the nebulizer is operated at an argon flow rate of  $1 \text{ L min}^{-1}$  and sample solution is delivered to the nebulizer by a peristaltic pump at a rate of  $0.36 \text{ mL min}^{-1}$ . The resulting spray is fed directly into the torch (i.e., no desolvation apparatus is employed).

To shield other instrumentation from RFI, a custom-designed copper housing enclosed the load coil, torch, nebulizer and spray chamber. Access ports for the necessary support facilities (i.e., argon gas, cooling water, drain, etc.) are provided and windows are cut into the housing for optical access. A piece of welding glass (O.D. 4) has been inserted into one window to enable the operator to monitor plasma operation.

Support Gas Handling. Delivery of the large quantities of prepurified argon gas (99.998%) needed to sustain the plasma requires a special gas handling system, a block diagram of which is shown in Figure 3. Three argon tanks are inter-connected by a manifold equipped with station and check valves (Matheson Gas Products, Joliet, Ill.). A single stage pressure regulator (Air Products, Allentown, Pa.) and a sensitive line regulator (Model 40H, Matheson Gas Products, Joliet, Ill.), combined in series, serve to reduce the tank pressure and maintain a constant upstream pressure. The argon gas is then delivered through toggle valves (Nupro Co., Cleveland, Ohio) to three rotameters (Series 7600, Matheson Gas Products, Joliet, Ill.). Each rotameter is equipped with a high accuracy needle valve (Series 4170, Matheson Gas Products, Joliet, Ill.) for controlling the rates at which argon is delivered to the nebulizer and torch.

Each rotameter tube was calibrated using a wet-test meter (Precision Scientific Co., Chicago, Ill.).

Optical Design. The entire optical system, the impedance matcher and plasma housing, and the monochromator are kinematically mounted onto an eight-foot lathe bed which serves as a optical support and alignment platform. As shown in Figure 1, optical radiation emitted in the tail flame of the plasma is collected by a 6-inch (15.2cm) spherically concave first-surface mirror (f.l. = 40.5cm, Al-MgF<sub>2</sub>/2000 coating, Oriel-Corp., Stamford, Conn.) which is held by a gimbal mount (Model 760, Newport Research Corp., Fountain Valley, Calif.). The light is imaged onto the entrance slit of a high resolution monochromator (magnification = 1.25) so the entire acceptance angle of the monochromator is filled. By rotating the mirror on its axes, the image of the plasma can be translated horizontally and vertically across the entrance slit to spatially select the region in the plasma being observed. The size of the observation region is thus determined by the width and height of the entrance slit. In preliminary tests and in routine use, this optical system was found to provide good spatial resolution and was simple to align and operate. In addition, the use of only one reflective surface to transfer the optical radiation from the plasma to the monochromator minimizes light losses and chromatic aberration. However, monochromatic aberrations (e.g., coma and astigmatism) can be a problem in such an off-axis system and careful attention must be paid to its design if high-fidelity imaging is desired (20,21). To reduce these aberrations, all off-axis angles should be minimized; in our system the off-axis angles employed limited spatial resolution to approximately 5mm in the plasma.

Detection System. Radiation transferred by the optical system is  
 ~~~~~  
 dispersed by a high resolution monochromator (Model HR1000, I.S.A. Inc., Metuchen, N.J.) employing a 120 X 140mm holographic grating with a groove density of  $2400 \text{ g mm}^{-1}$  and a reciprocal linear dispersion of  $3.9\text{\AA} \text{ mm}^{-1}$ . The dispersed radiation is detected by a photomultiplier tube (Model R636, Hamamatsu Corp., Middlesex, N.J.) operating at -1000 volts d.c. (Model 245 High Voltage Power Supply, Keithley Instruments Inc., Cleveland, Ohio) and mounted in a RFI-shielded housing (Model PR 1405, Products for Research Inc., Danvers, Mass.). The resulting photocurrent is monitored by a picoammeter (Model 414S, Keithley Instruments Inc., Cleveland, Ohio) which converts it into a proportional voltage. This voltage signal is passed through a variable time constant low-pass filter and displayed on a strip-chart recorder (Model SR204, Heath Company, Benton Harbor, Michigan).

#### Operating Procedure for Detection Limit Determinations.

~~~~~

Detection limits were determined for a number of elements using the experimental system just described and also with a conventional ICP torch (Model T-1, Plasma-Therm Inc., Kresson, N. J.). Typical operating conditions for both the mini and the conventional (maxi) ICP systems are outlined in Table I. Under these conditions, detection limits were determined using the following general operating procedure.

First, all electronic equipment including the RF generator was warmed up for at least one-half hour. The torch and nebulizer were then flushed with argon and the coolant and plasma gas flows cited on Table I were established.



These gas flows were found to provide the best conditions for stable plasma formation and operation. The slightly greater gas flows used in starting a plasma minimized the chances of torch damage during the ignition process. In the case of the mini-ICP the nebulizer gas flow could be set at approximately  $1 \text{ L min}^{-1}$  before plasma initiation while for the maxi-ICP the nebulizer gas must be initially shut off or the plasma could not be ignited. Next, the forward RF power level was set and the plasma ignited. After the plasma was formed, sample was introduced and the monochromator was scanned onto the peak of the analyte emission line of interest. Both observation height (defined as the vertical distance from the center of the observation zone to the top of the load coil) and sample introduction rate (i.e., nebulizer flow rate) were optimized for maximum signal-to-noise ratio for each element. At this point  $1 \mu\text{g mL}^{-1}$  sample solutions and blank solutions (i.e., distilled-deionized  $\text{H}_2\text{O}$ ) were alternately introduced; each signal was recorded 5 times for at least ten time constants each run. Signal-to-noise ratios were calculated from these measurements and detection limits were determined using the procedure described by Winefordner (22).

#### Plasma Excitation Temperature Measurements.

Excitation temperatures experienced by analyte species in both the mini and maxi ICP sources were determined using essentially the same experimental system and operating conditions as outlined above and in Table I. However, nebulizer gas flow rates were set at  $1.18 \text{ L min}^{-1}$  for the maxi-ICP and  $0.97 \text{ L min}^{-1}$  for the mini. In both cases the thermometric species (Fe) was

nebulized into the plasma as a  $1000 \mu\text{g mL}^{-1}$  solution. The relative intensities of the three Fe emission lines (cf. Table II) of interest were measured in the tail flames of both the maxi and mini plasmas at observation heights of 29.9 mm and 20.1 mm, respectively. The entrance slit width of the monochromator was decreased to 40  $\mu\text{m}$  for these measurements to ensure that the three Fe spectral lines were properly resolved. Spectral backgrounds at each emission line were measured while distilled-deionized water was aspirated into each plasma. The net emission line intensities of the Fe lines were determined by averaging three background-corrected values for each line.

#### Reagents.

~~~~~

Stock solutions were prepared as suggested by Dean and Rains (23), using reagent grade salts and acids as required. Analytical standards were prepared by suitable dilution of these stock solutions with freshly distilled-deionized water.

## RESULTS AND DISCUSSION

### Operating Characteristics of Mini-ICP.

RF Power. One of the anticipated advantages of the mini-ICP was its ability to perform usefully at reduced RF power levels. In our studies, the mini-ICP could easily be sustained with as little as 300 watts of forward RF power when no sample was introduced (Ar gas flows: coolant--7.9 L min<sup>-1</sup>, plasma--0.3 L min<sup>-1</sup>); moreover, while aqueous samples were being introduced, the mini-ICP remained stable with as little as 500 watts of RF power (Ar gas flows: coolant--9.8 L min<sup>-1</sup>, plasma--0 L min<sup>-1</sup>, nebulizer--0.68 L min<sup>-1</sup>). Significantly, these power levels do not represent the lowest possible but are only those at which the present mini-ICP system can easily operate; with improved torch and load coil configurations much lower operating levels should be obtainable.

In the present study, the mini-ICP was ordinarily operated at 1 kW (33% less RF power than the maxi); this value was selected on the basis of ease and stability of operation and on an approximate power density calculation. This calculation indicated that a 1 kW mini-plasma (10 mm diameter) would provide the same power density as a maxi-plasma (15 mm in diameter) operating at 1.5 kW. To perform this calculation the plasmas were modeled geometrically as toroids and a constant coupling efficiency was assumed (coupling efficiency is defined as the percentage of the RF power which is transferred from the load coil to the plasma).



Plasma Initiation and Sample Introduction. The ignition and stabilization  
~~~~~  
of a mini-plasma was found to be extremely simple using the operating procedure outlined earlier and under the conditions shown in Table I. Significantly, the mini-plasma could be ignited under either the operating or starting gas flows listed in Table I. Of course, the latter conditions would be preferable, because no flow adjustments would then be necessary between initiation and operation. However, occasionally (one of ten ignitions) torch damage occurred when "operating" (cf. Table I) gas flows were used during torch firing; to prolong the lifetime of the mini-torch, we ignite the plasma at the slightly higher (starting) gas flows. By comparison, damage to the maxi-torch occurred much more frequently (approximately one out of three times) when the plasma was initiated using the lower (operating) gas flows. Consequently, the maxi-plasma should only be ignited at the higher (starting) gas flows. In our experience, the lifetime of a mini-torch was much longer than a maxi, primarily because of the better stability of the mini-ICP during ignition. For example, during all our analytical investigations the same mini-torch was used while two maxi-torches suffered extensive damage.

The mini-plasma can also be struck while the nebulizer gas is flowing and distilled water is being aspirated, with an annular-shaped plasma being formed immediately. The entire plasma ignition and sample introduction process is thus very straightforward and could easily be automated. Importantly, only deionized-distilled water can be aspirated during plasma initiation, and instabilities result if a sample solution is aspirated at that time. In contrast, the maxi-ICP can not be initiated at all when the nebulizer gas is flowing. In fact, introducing sample into the maxi-plasma is not easily accomplished; it often causes plasma extinction and requires an operator with considerable experience.

Plasma Stability. After the mini-plasma is struck, it can be sustained  
 ~~~~~  
 easily for long periods of time, demonstrates excellent stability and accepts samples readily. Significantly, 50% less high-purity argon is consumed during this operation than with the conventional maxi-ICP (cf. Table I). The quantitative stability of the entire mini-plasma system is revealed by the reproducibility of the signal from a 1 ppm Fe solution, monitored at 3719.9Å. The signal was measured from a series of 5 sample and 5 blank solutions run over a 20 minute period, with a measurement time constant of one second. A relative standard deviation of 0.8% was calculated.

Sample Residence Time in Plasma. The velocity of sample injection into  
 ~~~~~  
 an ICP is significant, because it determines the time during which the analyte species can interact with the plasma. In turn, this interaction time should influence both the degree of matrix interferences and signal strength. Under the conditions listed in Table I, the injection velocity for the maxi-ICP was found to be 2806 cm sec<sup>-1</sup> and for the mini-ICP 3453 cm sec<sup>-1</sup>. Although these velocities are not the lowest usable with each plasma, it would not be surprising that the mini-plasma velocity is greater since higher injection velocities would be required to overcome the greater magnetohydrodynamic (MHD) thrust velocity expected in the mini-plasma (8,24).

Neglecting these potential MHD effects and assuming that the velocities of the particles remain constant and equal to the injection velocities, particle residence times will be approximately 1.5 milliseconds for the maxi-ICP and 0.8 milliseconds for the mini for observation heights of 30 mm and 20 mm respectively. These results suggest that higher regions of the mini-plasma might be optimum for observation; however, such is not the case as seen in

Figure 4B. From Figure 4B, analyte residence times are adequate for the analyte species to be efficiently desolvated, vaporized, atomized and excited.

**Background Spectra.** High-resolution recordings of the background radiation emitted by both the mini and the maxi ICP sources revealed highly structured spectra, containing many prominent features of both line and broad band character. The structure and intensities of the background spectra of the two sources were identical; however, their complex nature suggests that spectral interferences might be a problem for both sources. Studies directed at examining the mini-plasma's background in detail are currently underway in our laboratories.

#### Detection Limits.

A useful indication of the analytical utility of the mini-ICP can be obtained by comparing its limits of detection with those of a conventional maxi-ICP source. However, because detection limits are affected by every component in an AES system, comparisons between different systems are somewhat ambiguous. Consequently, detection limits were determined in this study for both a mini and a maxi ICP source on the same AES spectrometer (described in the Experimental section), and under essentially the same operating conditions (cf. Table I).

Detection limits for ten elements are listed in Table III. Because an uncertainty factor of 2 or 3 is inherent in detection limit determinations, the data in Table III indicate that the sensitivity available with a mini-ICP is comparable to that of a maxi-ICP. Significantly, the same detection limits



were obtained for both torches over a 4-month period, during which reproducibility checks were performed. Literature values are also listed in Table III and are comparable in most cases to those from the ICP-AES system described in this report.

#### Conditions for Simultaneous Multi-Element Analysis.

~~~~~

An important feature of ICP sources is their applicability to simultaneous multi-element analysis, a capability which is rendered more significant by the fact that a single set of operating conditions can be employed for a large number of elements (25). The results shown in Table III indicate that both the mini and maxi ICP sources can be used to determine a variety of elements with low limits of detection. However, these detection limits were not obtained under identical operating conditions; the observation height and nebulizer gas flows were optimized for each element.

The range of optimal conditions for different elements in ICP sources can be conveniently portrayed using diagrams like those of Boumans (25). Figures 4A and 4B are diagrams of this nature which illustrate the range of optimal conditions found for both the maxi and the mini ICP sources, respectively. These figures show that the choice of compromise conditions for the mini-ICP would be no more difficult than for the maxi-ICP.

In fact, compromise conditions may be easier to establish using the mini-ICP source. Figures 4A and 4B demonstrate that the range of optimal observation heights and nebulizer gas flows for different elements is smaller for the mini-ICP. As a result, compromise conditions can be selected which are closer to optimal for a larger number of elements in the mini-ICP than in the maxi-ICP.

### Excitation Temperatures.

Excitation temperatures of both mini and maxi ICP sources were determined using the Atomic Boltzmann Plot method (26,27), with neutral iron being used as the thermometric species (2). The wavelengths, excitation energies, statistical weights of the upper levels and relative transition probabilities of the appropriate lines are summarized in Table II.

From these measurements, an excitation temperature of 5054 °K is assigned to the maxi-ICP at an observation height of 30 mm and a 4295 °K temperature to the mini-ICP at an observation height of 20 mm. These observation regions are located in the cooler tail flames of the plasmas and represent the excitation temperatures experienced by analyte species during their observation. Although these observation heights differ by a factor of 1/3, so do the sizes of the two plasmas. Therefore, these temperatures should characterize the same relative regions in each source.

Because an uncertainty of 10% or more is usually associated with this type of measurement (2), the temperatures of the two plasmas can be assumed to be similar and agree with values determined by other workers (1,2). However, it would not be surprising for the mini-ICP to be slightly cooler than the maxi-ICP, in view of the different aerosol injection velocities of the two sources. This temperature similarity coupled with the similarity of the optimal observation regions for the mini and maxi plasmas (cf. Figures 4A and 4B) argues that the atomization and excitation behavior of the plasmas should not differ significantly.

### CONCLUSIONS

~~~~~

Through proper torch design and operation, a stable miniature inductively coupled plasma can be formed which readily accepts sample and exhibits many of the same analytical characteristics associated with conventional ICP sources. At present, it appears that the mini-ICP will be just as powerful a source for atomic emission spectrometry as conventional ICP sources while offering improved operating characteristics and reduced cost. Clearly, additional investigations into the analytical utility of this new source are warranted.

Experiments to examine the complete thermal nature of the mini-ICP are presently underway in our laboratories. The results of these investigations will provide insight into the physical nature of the source and the mechanisms controlling analyte atomization and excitation. Interference effects in conventional ICP sources have been shown to be minimal but when present they are complex and are directly related to the conditions under which they are generated (28-30). Future work will include a careful examination of the spectral, vaporization, and ionization interferences associated with the mini-ICP source. This area is particularly interesting because of the reduced residence times of the analyte species expected in the mini-ICP. In addition, progress is currently being made toward developing an improved miniature ICP source which will operate at even lower RF powers and reduced argon support gas flows.



## ACKNOWLEDGMENT

~~~~~

The authors are indebted to R. Cochran and M. Ramsey for their suggestions and constructive criticism in the course of this project. We also acknowledge with pleasure the assistance of E. Sexton in the design and construction of the miniature torch.

CREDIT  
~~~~~

Supported in part by the National Science Foundation through grant  
CHE 76-10896 and by the Office of Naval Research.

## LITERATURE CITED

~~~~~

- 1) D. J. Kalnicky, V. A. Fassel and R. N. Kniseley, Appl. Spectrosc., 31, 137 (1977).
- 2) D. J. Kalnicky, R. N. Kniseley and V. A. Fassel, Spectrochim. Acta, Part B, 30, 511 (1975).
- 3) K. Visser, F. M. Hamm and P. B. Zeeman, Appl. Spectrosc., 30, 34 (1976).
- 4) G. R. Kornblum and L. de Galan, Spectrochim. Acta, Part B, 32, 71 (1977).
- 5) G. W. Dickinson and V. A. Fassel, Anal. Chem., 41, 1021 (1969).
- 6) S. Greenfield, I. L. Jones, H. McD. McGeachin and P. B. Smith, Anal. Chim. Acta, 74, 225 (1975).
- 7) P. W. J. M. Boumans and F. J. de Boer, Spectrochim. Acta, Part B, 30, 309 (1975).
- 8) R. C. Miller and R. J. Ayen, J. Appl. Phys., 40, 5260 (1969).
- 9) R. N. Savage and G. M. Hieftje, to be submitted for publication.
- 10) T. B. Reed, J. Appl. Phys., 32, 2534 (1961).
- 11) S. Greenfield, I. L. Jones and C. T. Berry, Analyst, 89, 713 (1964).
- 12) S. Greenfield, H. McD. McGeachin and P. B. Smith, Talanta, 23, 1 (1976).
- 13) V. A. Fassel and R. N. Kniseley, Anal. Chem., 46, 1155A (1974).
- 14) P. W. J. M. Boumans, F. J. de Boer and J. W. de Ruiter, Philips Tech. Rev., 33, 50 (1973).
- 15) C. D. Allemand and R. M. Barnes, Appl. Spectrosc., 31, 434 (1977).
- 16) R. H. Scott, V. A. Fassel, R. N. Kniseley and D. E. Nixon, Anal. Chem., 46, 75 (1974).
- 17) R. H. Scott and M. L. Kokot, Anal. Chim. Acta, 75, 257 (1975).
- 18) J. L. Genna and R. M. Barnes, Anal. Chem., 49, 1450 (1977).
- 19) A. G. Gaydon and H. G. Wolfhard, "Flames," Chapman and Hall, Ltd., London, 1970.



- 20) S. A. Goldstein and J. P. Walters, Spectrochim. Acta, Part B, 31, 201 (1976).
- 21) S. A. Goldstein and J. P. Walters, Spectrochim. Acta, Part B, 31, 295 (1976).
- 22) J. D. Winefordner, P. A. St. John and W. J. McCarthy; Anal. Chem., 39, 1495 (1967).
- 23) J. A. Dean and T. C. Rains, "Standard Solutions for Flame Spectrometry," ch. 13 in "Flame Emission and Atomic Absorption Spectrometry," vol. 2, J. A. Dean and T. C. Rains, eds., Marcel Dekker, Inc., New York, N.Y., 1971, p. 332.
- 24) J. D. Chase, J. Appl. Phys., 42, 4870 (1971).
- 25) P. W. J. M. Boumans and F. J. de Boer, Spectrochim. Acta, Part B, 27, 391 (1972).
- 26) R. H. Tourin, "Spectroscopic Gas Temperature Measurements," Elsevier, New York, 1962, pp 47-48.
- 27) P. E. Walters, T. L. Chester and J. D. Winefordner, Appl. Spectrosc., 31, 1 (1977).
- 28) T. E. Edmonds and G. Horlick, Appl. Spectrosc., 31, 536 (1977).
- 29) G. R. Kornblum and L. de Galan, Spectrochim. Acta, Part B, 32, 455 (1977).
- 30) G. F. Larson, V. A. Fassel, R. H. Scott and R. N. Kniseley, Anal. Chem., 47, 238 (1975).
- 31) V. A. Fassel and R. N. Kniseley, Anal. Chem., 46, 1110A (1974).
- 32) I. Reif, "Spectroscopic Temperature Measurements of Flames and Their Physical Significance," PhD. Thesis, Iowa State University, Ames, Iowa (1971).

TABLE I. GENERAL OPERATING CONDITIONS FOR ICP-AES SYSTEM

|                                     | MAXI-ICP                                                                                                      | MINI-ICP |
|-------------------------------------|---------------------------------------------------------------------------------------------------------------|----------|
| RF Power <sup>a</sup>               | 1.5 kW                                                                                                        | 1.0 kW   |
| Gas Flows<br>(L min <sup>-1</sup> ) |                                                                                                               |          |
| Coolant (starting)                  | 18.4                                                                                                          | 9.8      |
| Coolant (operating)                 | 14.7                                                                                                          | 7.9      |
| Plasma (starting)                   | 1.1                                                                                                           | 0.3      |
| Plasma (operating)                  | 1.1                                                                                                           | 0        |
| Monochromator                       | Entrance slits = Exit slits<br>width = 50 $\mu$ m      width = 50 $\mu$ m<br>height = 5 mm      height = 5 mm |          |
| Time constant                       | 1 sec.                                                                                                        | 1 sec.   |

a) Forward power output from the RF generator.

TABLE II

## Fe EMISSION LINE DATA

| <u>Wavelength<br/>of Transi-<br/>tion, nm</u> | <u>Wavenumber<br/>of Emitting<br/>level, cm<sup>-1</sup></u> | <u>Statistical<br/>Weight of<br/>Upper Level</u> | <u>A<sub>λ</sub> (a)</u> |
|-----------------------------------------------|--------------------------------------------------------------|--------------------------------------------------|--------------------------|
| 382.043                                       | 33096                                                        | 9                                                | 3.91                     |
| 382.444                                       | 26140                                                        | 7                                                | 0.174                    |
| 382.588                                       | 33507                                                        | 7                                                | 3.48                     |

(a) Relative transition probability normalized to the Fe 371.994 nm line by  $A_{371.994} = 0.163$ ; taken from reference 32.



TABLE III COMPARISON OF DETECTION LIMITS<sup>a</sup> (ng mL<sup>-1</sup>)

| Element | Spectral line <sup>b</sup> | Maxi-ICP | Mini-ICP | Literature |
|---------|----------------------------|----------|----------|------------|
| Al      | 3961,5                     | 5        | 3        | 2 (5)      |
| Ca II   | 3933,7                     | 0,04     | 0,07     | 0,07 (31)  |
| Cd      | 2288,0                     | 13       | 42       | 30 (5)     |
| Cu      | 3247,5                     | 2        | 8        | 1 (31)     |
| Fe      | 3719,9                     | 12       | 10       | 5 (5)      |
| Mg      | 2852,1                     | 2        | 6        | 0,7 (31)   |
| Na      | 5889,9                     | 0,2      | 0,7      | 0,2 (31)   |
| Ni      | 3524,5                     | 15       | 4        | 6 (5)      |
| Pb      | 4057,8                     | 40       | 33       | 8 (5)      |
| Zn      | 2138,6                     | 23       | 71       | 10 (16)    |

a) Detection limits were defined as that concentration of analyte which produced a signal equal to 2.122 times the standard deviation of the blank signal. This factor was derived on the basis of five sample-background pair measurements and 99% confidence limits (22). See Table II for operating conditions.

b) Used in present study.

Figure 1. SCHEMATIC DIAGRAM OF ICP-AES EXPERIMENTAL SYSTEM  
(....) optical path; (---) electrical path; (—) gas flow

Figure 2. MINI-ICP TORCH CONSTRUCTION  
Quartz wall thickness = 1 mm. All features are drawn to scale.

Figure 3. BLOCK DIAGRAM OF ARGON GAS HANDLING SYSTEM

Figure 4. OPERATING CONDITIONS FOR GREATEST SIGNAL-TO-NOISE RATIO FOR SEVERAL ELEMENTS (a)

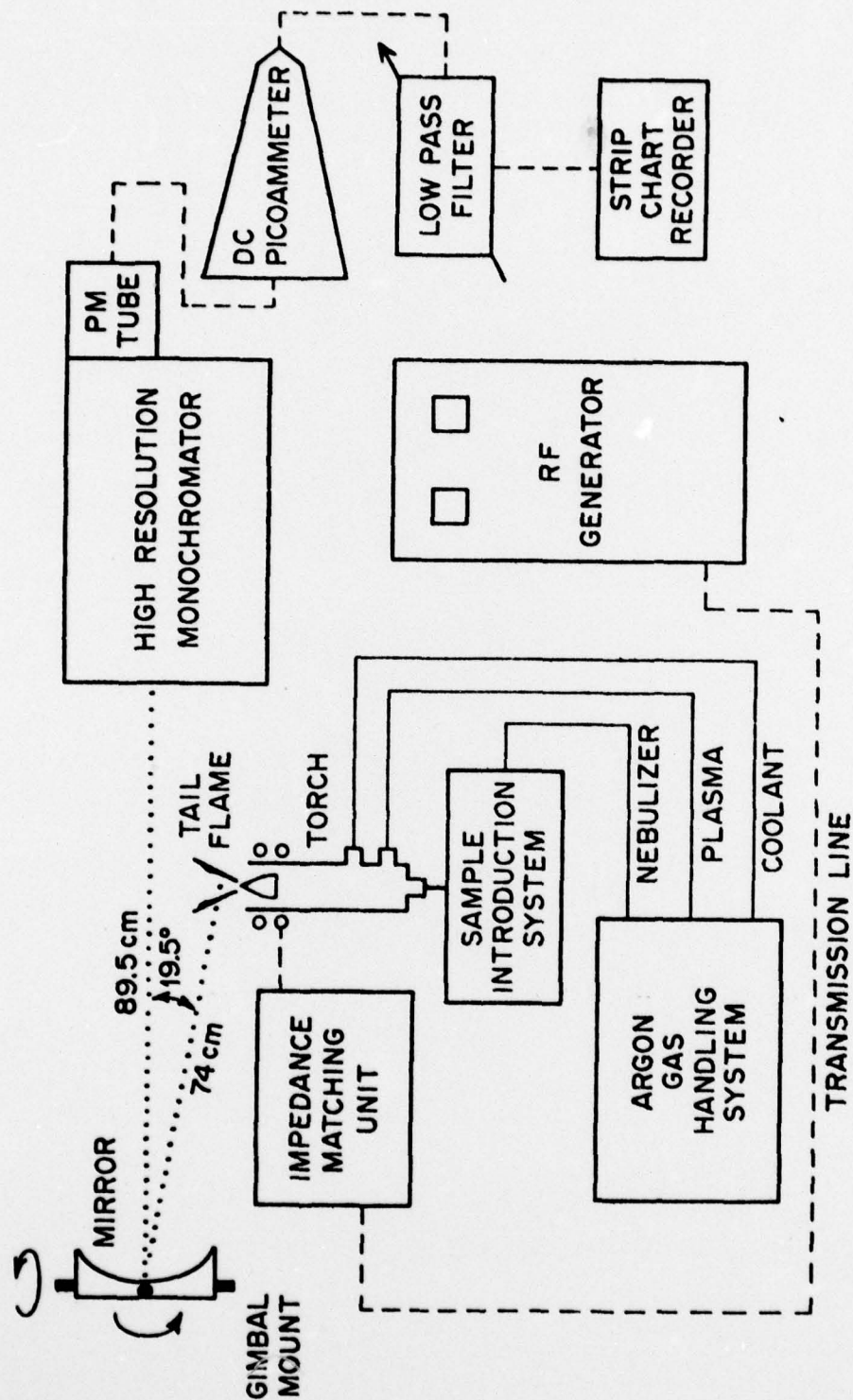
A Maxi-ICP

B Mini-ICP

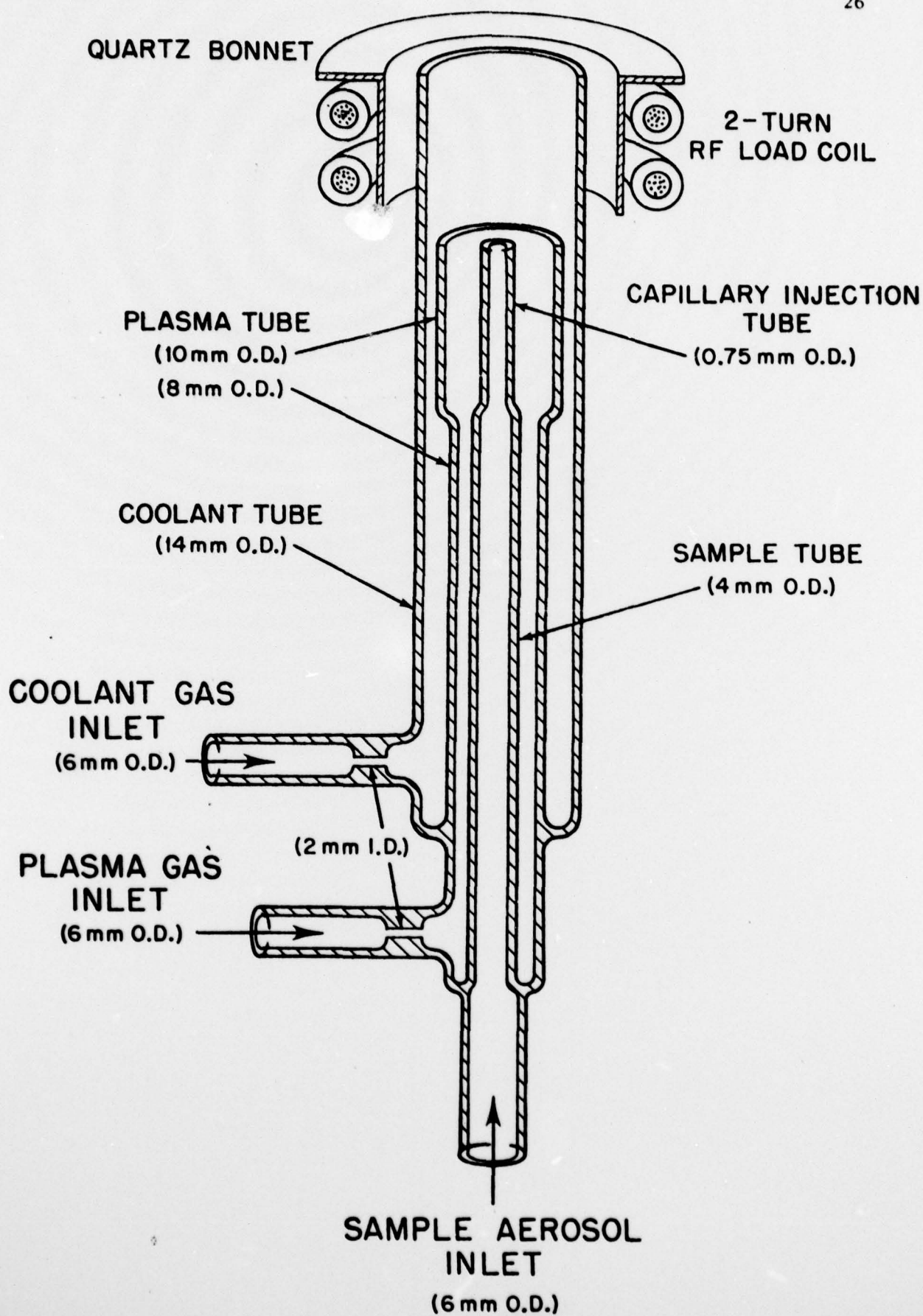
h = Height of observation zone (5 mm)

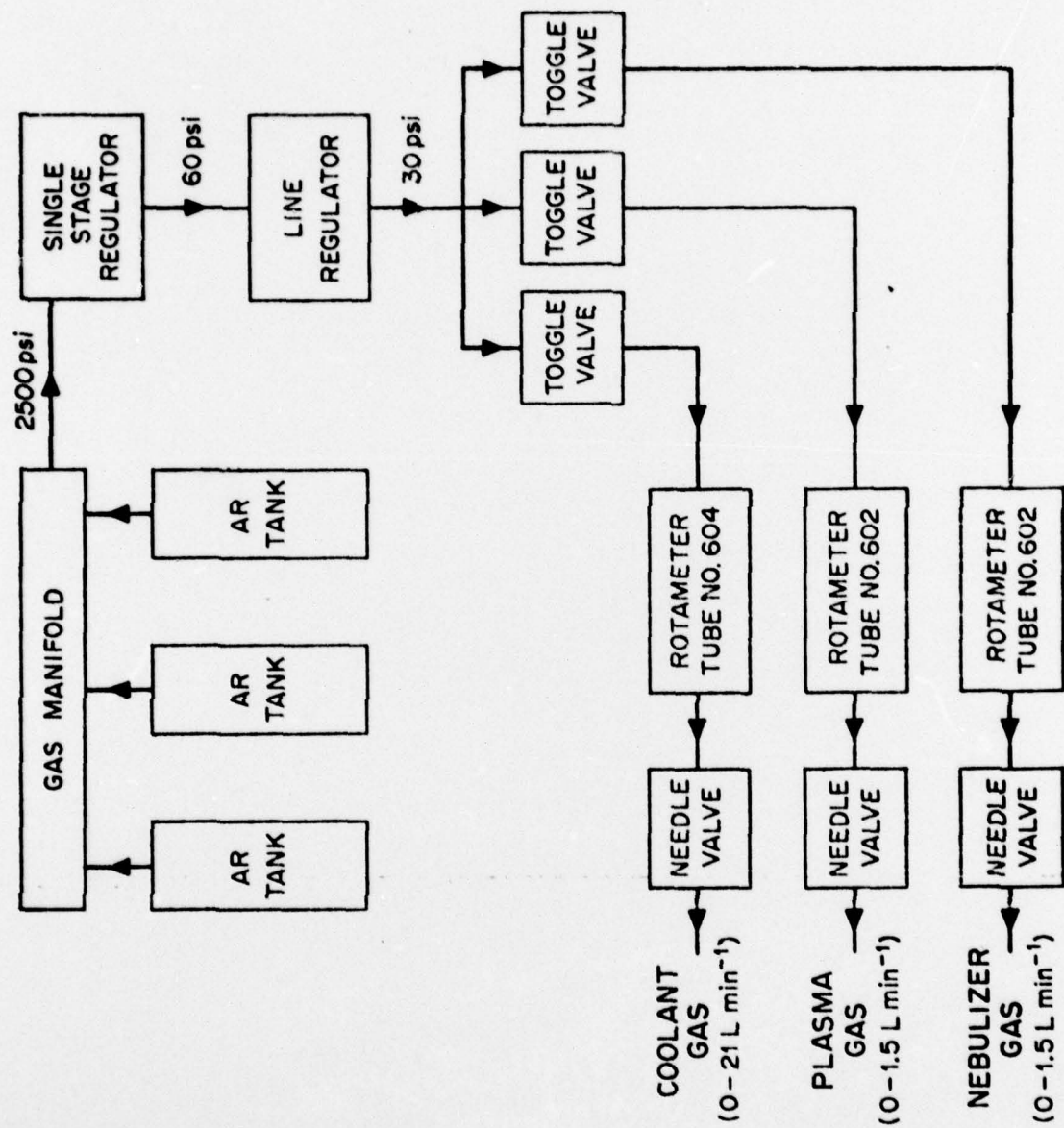
Over the entire range of conditions, measured detection limits for most elements changed by no more than a factor of 5, an amount considered insignificant in a practical analysis.

(a) After Boumans and DeBoer (25).

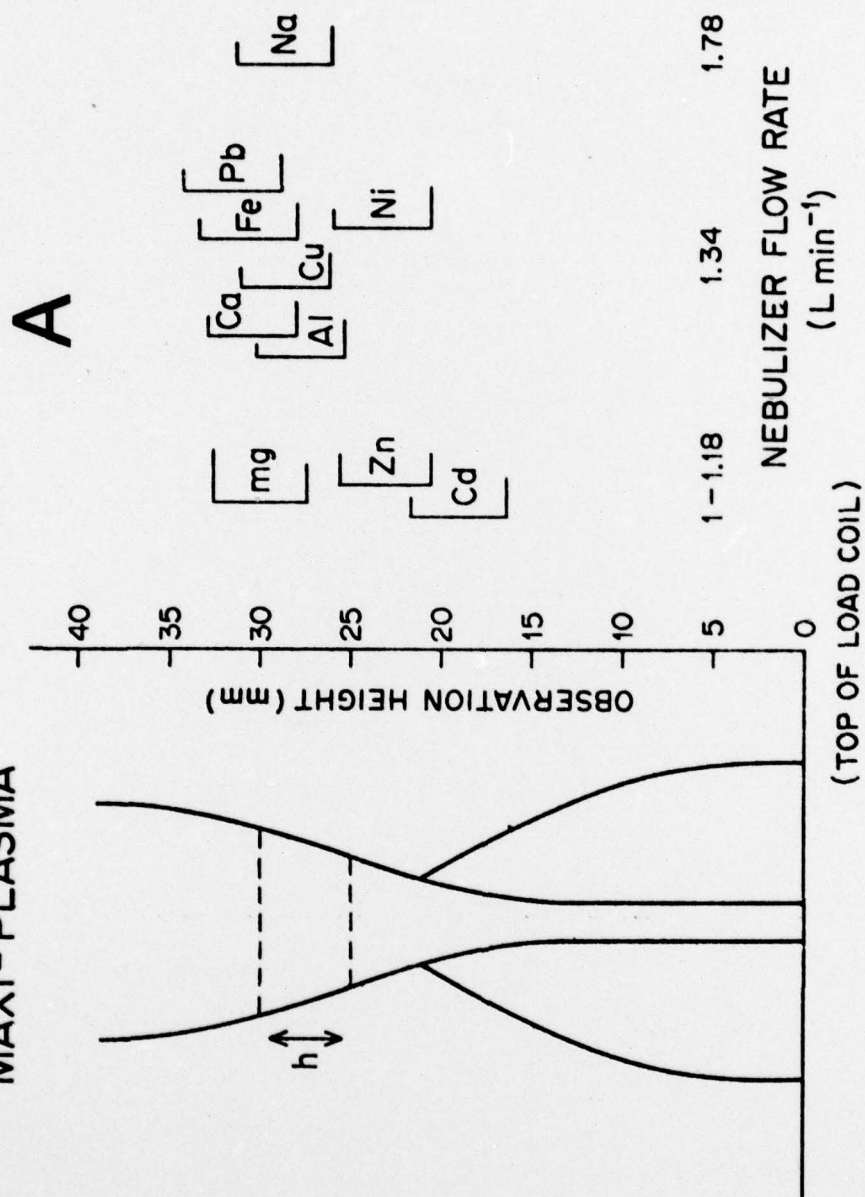






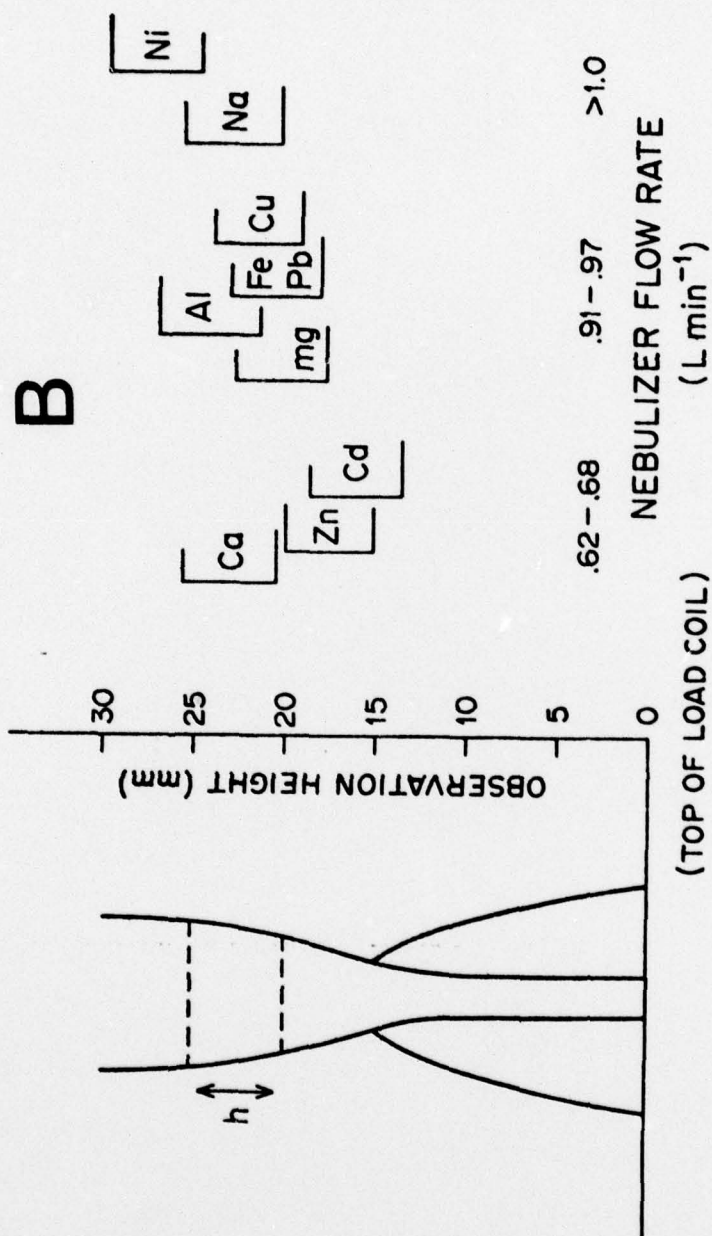


## MAXI-PLASMA





## MINI-PLASMA



# TECHNICAL REPORT DISTRIBUTION LIST

| <u>No. Copies</u> |                                                                                                                              | <u>No. Copies</u> |                                                                                                                    |
|-------------------|------------------------------------------------------------------------------------------------------------------------------|-------------------|--------------------------------------------------------------------------------------------------------------------|
| 2                 | Office of Naval Research<br>Arlington, Virginia 22217<br>Attn: Code 472                                                      | 12                | Defense Documentation Center<br>Building 5, Cameron Station<br>Alexandria, Virginia 22314                          |
| 1                 | ONR Branch Office<br>536 S. Clark Street<br>Chicago, Illinois 60605<br>Attn: Dr. Jerry Smith                                 | 1                 | U.S. Army Research Office<br>P.O. Box 12211<br>Research Triangle Park, N.C. 27709<br>Attn: CRD-AA-IP               |
| 1                 | ONR Branch Office<br>715 Broadway<br>New York, New York 10003<br>Attn: Scientific Dept.                                      | 1                 | Naval Ocean Systems Center<br>San Diego, California 92152<br>Attn: Mr. Joe McCartney                               |
| 1                 | ONR Branch Office<br>1030 East Green Street<br>Pasadena, California 91106<br>Attn: Dr. R. J. Marcus                          | 1                 | Naval Weapons Center<br>China Lake, California 93555<br>Attn: Head, Chemistry Division                             |
| 1                 | ONR Branch Office<br>760 Market Street, Rm. 447<br>San Francisco, California 94102<br>Attn: Dr. P. A. Miller                 | 1                 | Naval Civil Engineering Laboratory<br>Port Hueneme, California 93041<br>Attn: Mr. W. S. Haynes                     |
| 1                 | ONR Branch Office<br>495 Summer Street<br>Boston, Massachusetts 02210<br>Attn: Dr. L. H. Peebles                             | 1                 | Professor O. Heinz<br>Department of Physics & Chemistry<br>Naval Postgraduate School<br>Monterey, California 93940 |
| 1                 | Director, Naval Research Laboratory<br>Washington, D.C. 20390<br>Attn: Code 6100                                             | 1                 | Dr. A. L. Slafkosky<br>Scientific Advisor<br>Commandant of the Marine Corps (Code RD-1)<br>Washington, D.C. 20380  |
| 1                 | The Asst. Secretary of the Navy (R&D)<br>Department of the Navy<br>Room 4E736, Pentagon<br>Washington, D.C. 20350            | 1                 | Office of Naval Research<br>Arlington, Virginia 22217<br>Attn: Dr. Richard S. Miller                               |
| 1                 | Commander, Naval Air Systems Command<br>Department of the Navy<br>Washington, D.C. 20360<br>Attn: Code 310C (H. Rosenwasser) |                   |                                                                                                                    |

TECHNICAL REPORT DISTRIBUTION LIST

|                                                                                                                                          | <u>No. Copies</u> |                                                                                                                         | <u>No. Copies</u> |
|------------------------------------------------------------------------------------------------------------------------------------------|-------------------|-------------------------------------------------------------------------------------------------------------------------|-------------------|
| Dr. M. B. Denton<br>University of Arizona<br>Department of Chemistry<br>Tucson, Arizona 85721                                            | 1                 | Dr. Fred Saulfeld<br>Naval Research Laboratory<br>Code 6110<br>Washington, D.C. 20375                                   | 1                 |
| Dr. G. S. Wilson<br>University of Arizona<br>Department of Chemistry<br>Tucson, Arizona 85721                                            | 1                 | Dr. H. Chernoff<br>Massachusetts Institute of Technology<br>Department of Mathematics<br>Cambridge, Massachusetts 02139 | 1                 |
| Dr. R. A. Osteryoung<br>Colorado State University<br>Department of Chemistry<br>Fort Collins, Colorado 80521                             | 1                 | Dr. K. Wilson<br>University of California, San Diego<br>Department of Chemistry<br>La Jolla, California 92037           | 1                 |
| Dr. B. R. Kowalski<br>University of Washington<br>Department of Chemistry<br>Seattle, Washington 98105                                   | 1                 | Dr. A. Zirino<br>Naval Undersea Center<br>San Diego, California 92132                                                   | 1                 |
| Dr. I. B. Goldberg<br>North American Rockwell Science Center<br>P.O. Box 1085<br>1049 Camino Dos Rios<br>Thousand Oaks, California 91360 | 1                 | Dr. John Duffin<br>United States Naval Post Graduate School<br>Monterey, California 93940                               | 1                 |
| Dr. S. P. Perone<br>Purdue University<br>Department of Chemistry<br>Lafayette, Indiana 47907                                             | 1                 | <del>Dr. G. M. Hieftje<br/>Department of Chemistry<br/>Indiana University<br/>Bloomington, Indiana 47401</del>          | 1                 |
| Dr. E. E. Wells<br>Naval Research Laboratory<br>Code 6160<br>Washington, D.C. 20375                                                      | 1                 | Dr. Victor L. Rehn<br>Naval Weapons Center<br>Code 3813<br>China Lake, California 93555                                 | 1                 |
| Dr. D. L. Venezky<br>Naval Research Laboratory<br>Code 6130<br>Washington, D.C. 20375                                                    | 1                 | Dr. Christie G. Enke<br>Michigan State University<br>Department of Chemistry<br>East Lansing, Michigan 48824            | 1                 |
| Dr. H. Freiser<br>University of Arizona<br>Department of Chemistry<br>Tucson, Arizona 85721                                              |                   |                                                                                                                         |                   |